Episodic plate separation and fracture infill on the surface of Europa

Robert Sullivan*†, Ronald Greeley*, Kim Homan*, James Klemaszewski*, Michael J. S. Belton‡, Michael H. Carr§, Clark R. Chapman‖, Randy Tufts¶, James W. Head III#, Robert Pappalardo#, Jeffrey Moore☆, Peter Thomas & the Galileo Imaging Team**

* *Department of Geology, Box 871404, Arizona State University, Tempe, Arizona 85287-1404, USA*
‡ *National Optical Astronomy Observatory, Tucson, Arizona 85719, USA*
§ *US Geological Survey, Menlo Park, California 94025, USA*
‖ *Southwest Research Institute, Boulder, Colorado 8032, USA*
¶ *Lunar and Planetary Laboratory, University of Arizona, Tucson, Arizona 85721, USA*
# *Department of Geological Sciences, Brown University, Providence, Rhode Island 02912, USA*
☆ *Ames Research Center, Moffett Field, California 94035, USA*
** *Cornell University, Ithaca, New York 14853, USA*
† *Present address: 308 Space Sciences, Cornell University, Ithaca, New York 14853, USA*

Images obtained by the Voyager spacecraft revealed dark, wedge-shaped bands on Europa that were interpreted as evidence that surface plates, 50–100 km across, moved and rotated relative to each other[1]. This implied that they may be mechanically decoupled from the interior by a layer of warm ice or liquid water[2,3]. Here we report similar features seen in higher resolution images (420 metres per pixel) obtained by the Galileo spacecraft that reveal new details of wedge-band formation. In particular, the interior of one dark band shows bilateral symmetry of parallel lineaments and pit complexes which indicates that plate separation occurred in discrete episodes from a central axis. The images also show that this style of tectonic activity involved plates < 10 km across. Although this tectonic style superficially resembles aspects of similar activity on Earth, such as sea-floor spreading and the formation of ice leads in polar seas, there are significant differences in the underlying physical mechanisms: the wedge-shaped bands on Europa most probably formed when lower material (ice or water) rose to fill the fractures that widened in response to regional surface stresses.

Images of Europa obtained during the first and fourth orbits of the Galileo spacecraft around Jupiter show that a zone of dark, wedge-shaped bands seen obliquely in limited 2 km per pixel Voyager coverage extends WSW to about 40° S, 250° W in a prominent belt, 2,000 km by 600 km (Fig. 1). The zone is centred at about 15° S, 215° W, southwest of the anti-Jupiter point. Dark bands within this disrupted zone have other characteristic shapes besides wedges, including narrow crescents and trapezoids with maximum band widths of ~35 km. Contacts between dark band materials and surrounding brighter plains generally appear sharp at a resolution of 1.2–1.6 km per pixel (unlike the diffuse boundaries of triple bands revealed at the same resolution[4]). Sharply defined opposing margins of each dark band match closely in many instances, indicating that separation, translation and rotation (generally <10°) of icy plates occurred across areas now filled with dark band materials. This confirms, and expands to new areas of Europa, the conclusions of Schenk and McKinnon[2] that prominent dark bands making sharp contacts with brighter materials represent expressions of surface extension and plate separation.

A 420 m per pixel image obtained on orbit 3 reveals details of a prominent dark wedge band seen in Voyager 2 coverage. At Voyager resolution, dark wedge bands were reconstructed using single rotational or translational vectors to close each feature[2,3]. Higher-resolution Galileo data reveal that these features are much more complex, with each band involving many smaller plates moving individually or in groups (Fig. 2). Reconstruction across the most prominent dark band in the 420 m per pixel image, at 17° S, 197° W, cannot be accomplished using a single rotational or translational vector, but involves movement of at least 20 individual plates of bright plains material in a relatively small area. The northern 75 km of the band can be closed by ~18 km of ENE–WSW translation. The southern 105 km of the band can be closed by rotations of ~9° around a pole located at 21° S, 195° W. Two other, older bands, each with parallel lineaments in their interiors, can be closed with average plate translations of ~17 and 20 km. Cross-cutting relationships among these three dark bands indicate brightening to background terrain levels with increasing age, consistent with age/brightness trends of triple bands[4] and with the regional reconstruction of plates and stratigraphy in this area by Tufts *et al.*[5]. The two older bands could not be detected easily or evaluated using Voyager data, but clearly they contribute significantly to the structural history of the region, especially to the overall direction and amount of regional extension. Reconstruction of bright plates into pre-fractured configurations by dispensing with intervening dark material can be accomplished with little to no overlap of plate margins (Fig. 2), but a small fraction of bright plains material is missing and has somehow been consumed, or covered by or altered to darker materials. The small size of the plates allows the existence of viscous or liquid materials closer beneath the surface (at the time of plate movement) than would be suggested by the smallest plates visible at Voyager resolution. Many internal details are visible in the youngest of the three large dark bands, including: (1) interior lineaments that

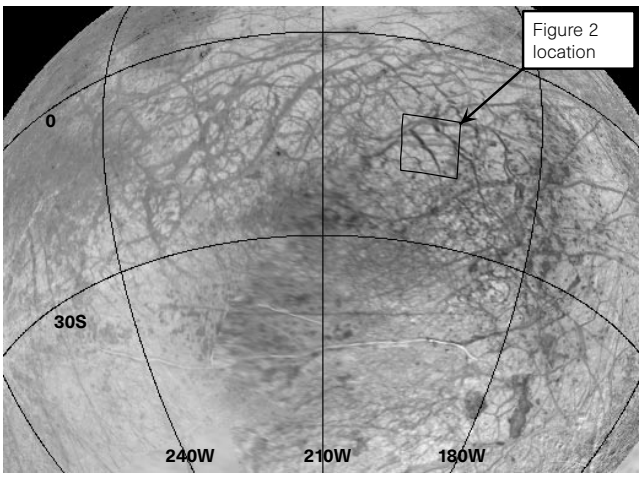

Figure 1 Combined Voyager and Galileo image data reprojected from above 40° S, 205° W. The location of the 420 m per pixel image in Fig. 2 is indicated. The 2,000-km belt of prominent dark, wedge-shaped bands extends in a south-facing crescent across the upper part of the figure. Bright plains marked with wedge-shaped bands partially surround a densely fractured region centred at 40° S, 205° W. Scale: 30° of latitude = 820 km.

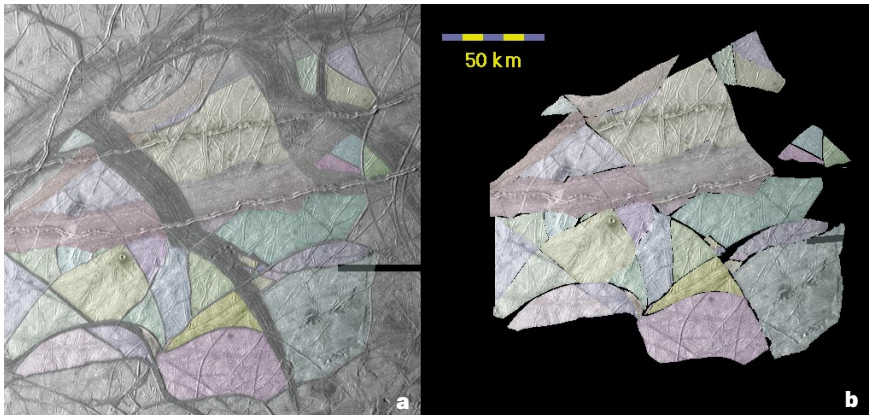

Figure 2 Part of Galileo image S0368639400 of Europa, with north up. In this area plates of bright plains materials, some <10 km across, can be fitted together with no overlap by dispensing with intervening dark materials. Twenty individual bright plates involved in closing the prominent dark, wedge-shaped band in the centre of **a** have been tinted to demonstrate reconstruction with no plate overlap in **b**.

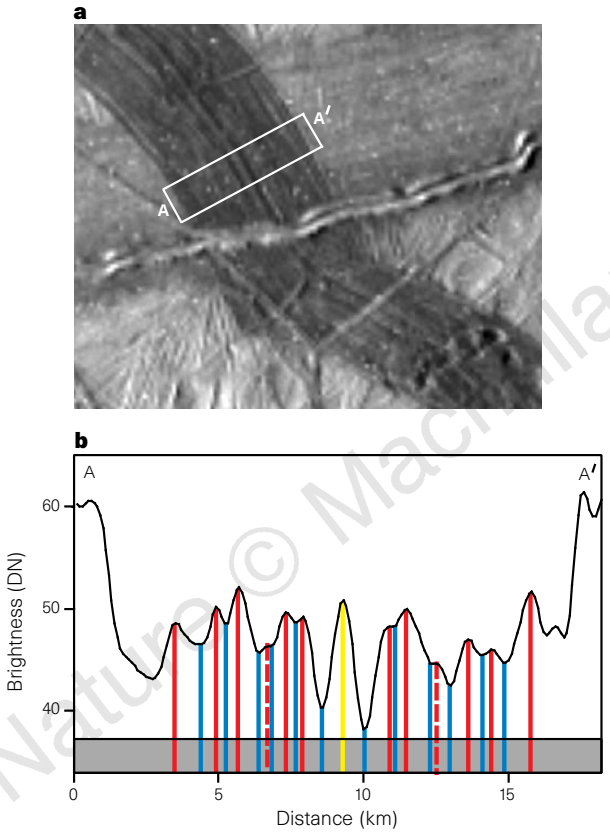

Figure 3 Bilateral symmetry of internal details within the dark, wedge-shaped band shown in Fig. 2. Enlargement (with interpolation/smoothing) in **a** of the view in Fig. 2 shows parallel internal lineaments and mirrored arrangements of four pits (southeast) in the dark band. An averaged brightness profile in units of image data numbers (DN) from A to A′ is shown in **b**, where the locations of convex-up and concave-up inflections are marked in red and blue, respectively. Minor inflections (dashed) are less certain. The order of brightness inflections in the grey strip along the bottom of the plot is symmetric around the central axis of the band, marked by the yellow line.

parallel band margins and each other; (2) a central lineament pair; and (3) bilateral symmetry of some features, including prominent internal lineaments, brightness inflections, and pit complexes (Fig. 3). Narrower dark bands seen in the image lack many or all of these characteristics at available resolution, and have neutral or positive relief.

Bilateral symmetry of some features within the youngest dark band is consistent with repeated emplacement of materials primarily at the centre of the band, with material moving to each side to make way for newer material rising from below as the bright plates moved further apart. Lineaments closer to the centre of the band trace a more rounded version of the band margins, indicating intervals of inactivity long enough for structural adjustments to occur which affected the trend of succeeding spreading episodes. Internal ridges and troughs (and more subtle brightness inflections that are probably due to poorly resolved ridge and trough topography) indicate that dark materials were emplaced at the centre of the band with substantial viscosity, or became highly viscous rapidly enough after emplacement to retain structure while migrating from the band axis. Consistent with this are the much narrower bands of dark material in the 420 m per pixel image that stand tends of metres above the bright plates they divide, indicating they were extruded too viscously to flow onto surrounding terrain. It is unclear from the image whether or not deeper material rose in a viscous state as well. (If it did, viscosity of material rising towards the central axis of the band could gradually have imposed a slightly more efficient conduit configuration with a straighter trend between the band margins, resulting in the observed rounding of the trend of the band axis with time.) An alternative terrestrial sea-ice analogy involving repeated opening and refreezing of 'leads' of liquid water must still account for the incremental emplacement of dark material in discrete episodes along a central axis, and in this model progressive straightening of the axis with time is harder to explain. These issues can only be settled when very high-resolution images are obtained over this feature later in the Galileo mission; but in any case, the dark band materials are shown to be capable of plastic flow around very small bright plates, only a few kilometres across, that remain undeformed by the process. This implies that deformable material, such as plastically deforming ice or liquid water, was present at depths on the same scale as the smallest plate dimensions. The small percentage of missing (or darkened) bright plate material in the reconstruction contrasts with areas of chaos on Europa such as Conamara, where breakup of icy crust into mobile plates occurred with significant collateral destruction of plate material (perhaps including subsidence and burial) and replacement by a chaotic matrix of icy rubble that might have been emplaced fluidly[6]. In those regions crust was destroyed and/or buried during resurfacing, while in the 2,000-km belt of dark bands crust was created seemingly to fill gaps that opened between preserved, undeformed plates.

Dark bands with matching sharp margins provide good evidence for crustal extension in these areas, but so far there is no clear evidence of corresponding zones where bright plate material was consumed with the growth of dark bands. The close fit obtained when bright plates are reassembled implies that their shapes and surface areas remained relatively constant during spreading, so features analogous to terrestrial subduction zones should not be expected within the bright plates. The possibility that dark bands might at times alternate as sites of convergence, closure, and

consumption of surface materials cannot be ruled out, but the apparent lack of convergence zones is one of several important differences between plate tectonics on Earth and what has been seen so far of plate movement and dark band growth on Europa.

Even without surface signatures of plate convergence, could the ~100-km spacing of the more prominent dark bands (Fig. 1) be a result of subsurface convection that does not, or did not, involve recycling of surface materials? If so, this would be on a different scale to solid-state convection proposed near Conamara Chaos[7]. In that area Pappalardo *et al.*[7] conclude that domes, dark spots, and pits are evidence for thermally driven vertical movements 7–15 km in diameter and 5–20 km apart in the near-subsurface. Domes, dark spots, and pits are much less pervasive among the dark wedge bands discussed here, suggesting that heat transfer from the interior occurred differently in this area. Although a water-ice-rich layer >50 km thick is allowed by several analyses that assume differentiation and segregation of water from a deeper silicate mantle[8,9], as well as interior models based on gravitational data derived from Doppler tracking of the Galileo spacecraft[10], the idea that these materials are organized into a network of ~100-km convection cells causing dark band formation is inconsistent with the existence of isolated dark wedge bands (for example, near 52° N, 230° W).

A more likely explanation is that plate fracturing and movement in response to regional surface stresses simply allowed material to rise passively to the surface to form the dark bands. A very densely fractured region centred at 40° S, 205° W is partly surrounded by bright plains with prominent dark bands showing evidence of plate offsets[1–3,11–13] (Fig. 1). This annulus includes the disrupted zone seen by Galileo on its first and fourth orbits and the dark bands seen at higher resolution on the third orbit. Destruction of surface material in the area of 40° S, 205° W could have provided room in surrounding terrain for icy plates to separate and rotate relative to one another, with emplacement of dark band material between the plates occurring in response to these motions. The very densely fractured region in the centre of the annulus has not been seen yet at high resolution, so the cause of the dense fracturing and the fate of the original surface materials cannot be determined. Localized heating similar to that proposed for the Conamara Chaos region[6] is a likely possibility. We conclude that creation of dark bands during plate separation is a result of regional surface stresses opening pre-existing fractures which sub-surface materials exploit incrementally. □

Received 26 August; accepted 11 December 1997.

1. Schenk, P. M. & Seyfert, C. K. Fault offsets and proposed plate motions for Europa. *Eos* **61,** 286 (1980).
2. Schenk, P. M. & McKinnon, W. B. Fault offsets and lateral crustal movement on Europa: Evidence for a mobile ice shell. *Icarus* **79,** 75–100 (1989).
3. Golombek, M. P. & Banerdt, W. B. Constraints on the subsurface structure of Europa. *Icarus* **83,** 441–452 (1990).
4. Belton, M. J. S. *et al.* Galileo's first images of Jupiter and the Galilean satellites. *Science* **274,** 377–385 (1996).
5. Tufts, B. R., Greenberg, R., Sullivan, R., Pappalardo, R. & the Galileo Imaging Team Reconstruction of Europan terrain in the Galileo C3 "wedges" image and its geological implications. *Lunar Planet. Sci. Conf.* **XXVIII,** 1455–1456 (1997).
6. Carr, M. H. *et al.* Evidence for a subsurface ocean on Europa. *Nature* **391,** 363–365 (1998).
7. Pappalardo, R. T. *et al.* Morphological evidence for solid-state convection in Europa's ice shell. *Nature* **391,** 365–368 (1998).
8. Fanale, F. P., Johnson, T. V. & Matson, D. L. in *Planetary Satellites* (ed. Burns, J. A.) 379–405 (Univ. Arizona Press, Tucson, 1977).
9. Squyres, S. W., Reynolds, R. T., Cassen, P. M. & Peale, S. J. Liquid water and active resurfacing on Europa. *Nature* **301,** 225–226 (1983).
10. Anderson, J. D., Lau, E. L., Sjogren, W. L., Schubert, G. & Moore, W. B. Europa's differentiated internal structure: Inferences from two Galileo encounters. *Science* **276,** 1236–1239 (1997).
11. Tufts, B. R. Photogeological analysis of Europan tectonic features. *Lunar Planet Sci. Conf.* **XXIV,** 1445–1446 (1993).
12. Tufts, B. R. A San Andreas-sized strike-slip fault on Europa. *Lunar Planet Sci. Conf.* **XXVII,** 1343–1344 (1996).
13. Pappalardo, R. T. & Sullivan, R. Evidence for separation across a gray band on Europa. *Icarus* **123,** 557–567 (1996).

Acknowledgements. We thank N. Sleep for reviews, and K. Klaasen, H. Breneman, T. Jones, J. Kaufman, K. Magee and D. Senske at JPL for their efforts. Cooperation from personnel responsible for other instruments after a playback anomaly on Galileo's third orbit allowed recovery of the high-resolution image shown in Figs 2 and 3. This work was supported by NASA's Galileo Project.

Correspondence and requests for materials should be addressed to R.S. (e-mail: sullivan@cuspif.tn.cornell.edu).

Transport properties governed by surface barriers in $Bi_2Sr_2CaCu_2O_8$

Dan T. Fuchs*, Eli Zeldov*, Michael Rappaport†, Tsuyoshi Tamegai‡, Shuuichi Ooi‡ & Hadas Shtrikman*

* *Department of Condensed Matter Physics,* † *Physics Services, The Weizmann Institute of Science, Rehovot 76100, Israel*

‡ *Department of Applied Physics, The University of Tokyo, Hongo, Bunkyo-ku, Tokyo 113, Japan*

One of the most common investigation techniques of type-II superconductors is the transport measurement, in which an electrical current is applied to a sample and the corresponding resistance is measured as a function of temperature and magnetic field. At temperatures well below the critical temperature, T_c, the resistance of a superconductor is usually immeasurably low. But at elevated temperatures and fields, in the so-called vortex liquid phase, a substantial linear resistance is observed[1]. In this dissipative state, which in anisotropic high-temperature superconductors like $Bi_2Sr_2CaCu_2O_8$ may occupy most of the mixed-state phase diagram, the transport current is usually assumed to flow uniformly across the sample as in a normal metal. To test this assumption, we have devised a measurement approach which allows determination of the flow pattern of the transport current across the sample. The surprising result is that, in $Bi_2Sr_2CaCu_2O_8$ crystals, most of the current flows at the edges of the sample rather than in the bulk, even in the highly resistive state, due to the presence of strong surface barriers. This finding has significant implications for the interpretation of existing resistivity data and may be of importance for the development of high-temperature superconducting wires and tapes.

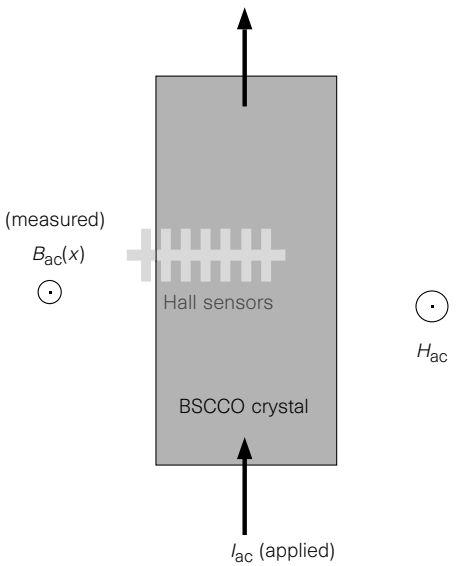

Figure 1 Experimental set-up. A schematic top view of $Bi_2Sr_2CaCu_2O_8$ crystal ($1.5 \times 0.15 \times 0.01$ mm) attached to an array of seven GaAs/AlGaAs two-dimensional electron-gas Hall sensors underneath the sample. The sensors have an active area of $10 \times 10\,\mu m^2$ and are 10 μm apart. There is one sensor outside the sample; the other six span more than half of the sample width. Magnetic field H_{dc} is applied perpendicular to the sample surface. An a.c. current I_{ac} is applied to the crystal through electrical contacts. The sensors are used to probe the perpendicular component of the self-induced a.c. field, B_{ac}, generated by the a.c. current.